Draft version February 22, 2018
Preprint typeset using LaTeX style emulateapj v. 08/22/09

LYα ABSORBERS DO/NOT CO-ROTATE WITH GALAXY DISKS

David M. French, Bart P. Wakker
Department of Astronomy, University of Wisconsin, Madison, WI 53706, USA
Draft version February 22, 2018

ABSTRACT

We present results of a study comparing the relative velocity of Lyα absorbers to the rotation direction and velocity of nearby galaxy disks. We find...

Subject headings: galaxies:intergalactic medium, galaxies:evolution, galaxies:halos, quasars: absorption lines

1. INTRODUCTION

Galaxy rotation curves have been observed to extend at constant velocity out to... (cite...). It becomes increasingly difficult to measure gas rotation much farther from this however as the density rapidly decreases. Within this region the galaxy disks transition into circumgalactic medium (CGM), and eventually the CGM merges with the intergalactic medium (IGM). At what point, however, does the surrounding medium cease to circulate with the galaxy? Stewart et al. (2011) suggests through (HYDRO?) simulations that the bulk CGM kinematics out to (WHAT DISTANCE) may circulate, and that absorption in intervening QSO sightlines should be able to accurately capture this rotation signature.

There have been several studies with a sample size of 1 or a few aiming to compare the kinematics of the galaxy disk to absorption detected in it's CGM halo (e.g., Cote et al. 2005; Wakker & Savage 2009; Bowen et al. 2016; **MORE**). With these individual results we may be missing the forest for the sake of the individual trees. There has yet to be a more systematic search for observational evidence that the CGM is kinematically associated with galaxies in general.

Numerous studies have shown a correlation between equivalent width and decreasing velocity difference between galaxies and IGM absorbers (e.g., French & Wakker 2017, MORE).

To make progress here, we have obtained rotation curves for 12 nearby spiral galaxies which are located within 500 kpc of a background QSO observed by the Cosmic Origins Spectrograph (COS) on *HST*.

2. DATA AND ANALYSIS

2.1. *SALT Data*

Our sample contains 12 galaxies observed with the Southern African Large Telescope (SALT) Robert Stobie Spectrograph (RSS) in longslit mode. These 12 were selected from a larger pool of 48 submitted targets by the SALT observing queue. These 48 possible targets were chosen for their proximity to background QSOs whose spectra contained promising Lyα lines. Finally, we only included galaxies with $z \leq 0.33$ ($cz \leq 10,000$ km s^{-1}), angular sizes less than 6' to ensure easy sky subtraction, and surface brightnesses sufficient to keep exposure times below 1300s. Table 2 summarizes these observations. Data was taken for 2 additional galaxies, NGC3640 and NGC2962, but proved unusable due to issues with spectral identification and low signal to noise (respectively).

All SALT galaxy spectra were reduced and extracted using the standard PySALT reduction package (**CITATION**), which includes procedures to prepare the data, correct for gain, cross-talk, bias, and overscan, and finally mosaic the images from different extensions. Next, we rectify the images with wavelength solutions found via Ne and Ar arc lamp spectra line identification. Finally, we perform a basic sky subtraction using an off-sky portion of the image, and extract 5-10 pixel wide 1-D strips from the reduced 2-D spectrum.

For each 1-D spectrum, we identify the Hα emission lines and perform a non-linear least-squares Voigt profile fit using the Python package LMFIT[1]. The line centroid and 1σ standard errors are returned, and these fits are then shifted to rest-velocity based on the galaxy systemic redshift and heliocentric velocity corrections are calculated with the IRAF rvcorrect procedure. The final rotation velocity is calculated by then applying the inclination correction, $v_{rot} = v/\sin(i)$. Final errors are calculated as

$$\sigma^2 = \left(\frac{\partial v_{rot}}{\partial \lambda_{obs}}\right)^2 (\Delta\lambda_{obs})^2 + \left(\frac{\partial v_{rot}}{\partial v_{sys}}\right)^2 (\Delta v_{sys})^2 + \left(\frac{\partial v_{rot}}{\partial i}\right)^2 (\Delta i)^2, \quad (1)$$

where $\Delta\lambda_{obs}$, Δv_{sys}, and Δi are the errors in observed line center, galaxy redshift, and inclination, respectively. We determine the inclination error by calculate the standard deviation of all axis ratio values available for each galaxy in NED. The final physical scale is calculated using the SALT image scale of 0.1267 arcsec/pixel, multiplied by the 4-pixel spatial binning, and converted to physical units using a redshift-independent distance if available, and a Hubble flow estimate if not. We adopt a Hubble constant of $H_0 = 71$ km s^{-1}Mpc^{-1} throughout.

Finally, we calculate our approaching and receding velocities via a weighted mean of the outer 1/2 of each rotation curve, with errors calculated as weighted standard errors in the mean. Our final redshifts are calculated by forcing symmetric rotation, such that the outer 1/2 average velocity for each side matches. See Figure **??** for an example.

[1] `http://cars9.uchicago.edu/software/python/lmfit/contents.html`

Target	R.A.	Dec.	z	Program	Grating	Obs ID	Obs Date	T_{exp}* [ks]	S/N* [1238]
(1)	(2)	(3)	(4)	(5)	(6)	(7)	(8)	(9)	(10)
1H0717+714	7.0 21.0 53.3	71.0 20.0 36.0	0.5003	12025	G130M	LBG812	11-12-27	6.0	37

Table 1
COS targets in this sample. *Total exposure time and S/N ratio is given for multi-orbit exposures.

.

Galaxy	R.A.	Dec.	cz (km s^{-1})	Type	Grating	V$_{\rm rot}$ [km s^{-1}]	V$_{\rm rot}$/ sin(i) [km s^{-1}]	Obs Date	T_{exp} [ks]
(1)	(2)	(3)	(4)	(5)	(6)	(7)	(8)	(9)	(10)
CGCG039-137	11 21 26.95	+03 26 41.68	6918 ± 24	Scd	PG2300	132 ± 16	139 ± 26	05 11 2016	700
IC5325	23 28 43.43	−41 20 0.49	1512 ± 8	SAB(rs)bc	PG2300	53 ± 5	125 ± 39	05 17 2016	600
MCG-03-58-009	22 53 40.85	−17 28 44.00	9015 ± 19	Sc	PG2300	150 ± 12	171 ± 23	05 16 2016	1200
NGC1566	04 20 0.42	−54 56 16.12	1502 ± 15	SAB(rs)bc	PG2300	64 ± 8	195 ± 47	10 18 2016	400
NGC3513	11 03 46.08	−23 14 43.8	1204 ± 12	SB(s)c	PG2300	11 ± 10	22 ± 24	05 26 2016	600
NGC3633	11 20 26.22	+03 35 8.20	2587 ± 7	SAa	PG2300	149 ± 6	157 ± 9	05 11 2016	1200
NGC4536	12 34 27.05	+02 11 17.30	1867 ± 33	SAB(rc)bc	PG2300	129 ± 9	148 ± 41	05 11 2016	1300
NGC4939	13 04 14.39	−10 20 22.60	3093 ± 33	SA(s)bc	PG2300	204 ± 25	275 ± 66	05 14 2016	500
NGC5364	13 56 12.00	+05 00 52.09	1238 ± 17	SA(rs)bc pec	PG2300	130 ± 13	155 ± 22	05 11 2016	700
NGC5786	14 58 56.26	−42 00 48.10	2975 ± 22	SAB(s)bc	PG2300	156 ± 10	172 ± 25	05 11 2016	250
RFGC3781	21 37 45.18	−38 29 33.22	9139 ± 32	Sb	PG2300	203 ± 32	203 ± 32	05 16 2016	1000
UGC09760	15 12 02.44	+01 41 55.46	2094 ± 16	Sd	PG2300	46 ± 10	46 ± 16	05 11 2016	500

Table 2
SALT targeted galaxies. Columns are as follows: 1) the galaxy name, 2), 3) R.A., Dec. in J2000, 4) galaxy systemic velocity, 5) morphological type (RC3), 6) RSS grating used, 7) approaching side velocity, 8) receding side velocity, 9) observation date, 10) exposure time, and 11) S/N of the Hα or Ca H&K lines.

2.2. *COS Spectra*

3. SALT GALAXIES

3.0.1. *CGCG039-137*

Systemic velocity as published: 6902 Velocity as measured: 6917.8 ± 23.7 Rotation velocity (inc corrected) 139 ± 26 km s^{-1}Rotation velocity (observed) 132 ± 16 km s^{-1}Inclination: 61 Adjusted Inc: 63 Morphology:

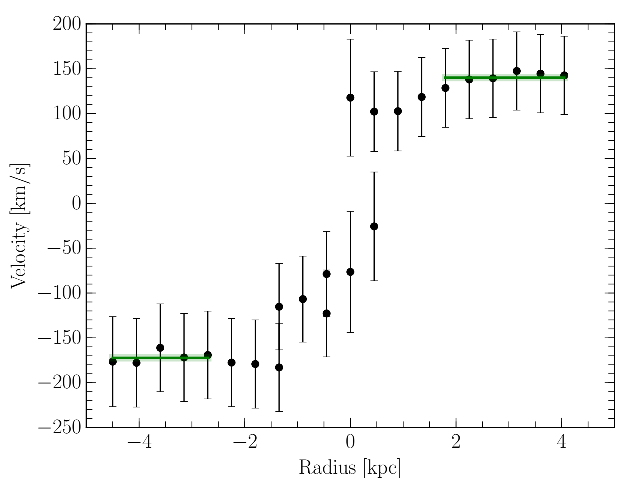

Figure 1. Rotation curve of NGC3633. The solid green line indicates the weighted mean velocity over the corresponding x-axis region, and the shaded green indicates the 1σ error in the mean.

Scd $L_* = 0.62$

Two sightlines:
RX_J1121.2+0326 at 99 kpc, 71deg az:
6975 Lya (dv = 75 km s^{-1}on pos side)
SDSSJ112224.10+031802.0 at 491 kpc, 24deg az :
6606 Unmarked (dv = -312 km s^{-1}on neg side)

3.0.2. *ESO343-G014*

Systemic velocity as published: 9162 Velocity as measured: 9138.9 ± 31.7 Rotation velocity (inc corrected) 205 ± 53 km s^{-1}Rotation velocity (observed) 203 ± 6 km s^{-1}Inclination: 84 Adjusted Inc: 90 Morphology: Sb $L_* = 1.1$

One sightline:
RBS1768 at 466 kpc, 74deg az:
9308 Lya (dv = 169 km s^{-1}on pos side) 9360 Lya (dv = 221 km s^{-1}on pos side) 9434 Lya (dv = 295 km s^{-1}on pos side)

3.0.3. *IC5325*

Systemic velocity as published: 1503 Velocity as measured: 1511.9 ± 8.4 Rotation velocity (inc corrected) 125 ± 45 km s^{-1}Rotation velocity (observed) 53 ± 5 km s^{-1}Inclination: 25 Adjusted Inc: 25 Morphology: SAB(rs)bc $L_* = 0.9$

One sightline:
RBS2000 at 314 kpc, 64deg az:
1598 Lya (dv = 86 km s^{-1}on possibly? neg side)

3.0.4. *MCG-03-58-009*

Systemic velocity as published: 9030 Velocity as measured: 9014.9 ± 18.6 Rotation velocity (inc corrected) 171 ± 24 $\mathrm{km\,s^{-1}}$Rotation velocity (observed) 150 ± 12 $\mathrm{km\,s^{-1}}$Inclination: 48 Adjusted Inc: 49 Morphology: Sc $L_* = 2.9$

One sightline:
MRC2251-178 at 355 kpc, 71deg az:
9029 Lya (dv = 14 $\mathrm{km\,s^{-1}}$on pos side)

3.0.5. *NGC1566*

Systemic velocity as published: 1504 Velocity as measured: 1501.9 ± 14.9 Rotation velocity (inc corrected) 86 ± 21 $\mathrm{km\,s^{-1}}$Rotation velocity (observed) 64 ± 13 $\mathrm{km\,s^{-1}}$Inclination: 46 Adjusted Inc: 48 Morphology: (R'_1)SAB(rs)bcSy1 $L_* = 0.59$ Four sightlines: 1H0419-577 at 303 kpc, 10deg az:
1071 Lya (dv = -427 $\mathrm{km\,s^{-1}}$on pos side) 1123 Lya (dv = -379 $\mathrm{km\,s^{-1}}$on pos side) 1188 Lya (dv = -314 $\mathrm{km\,s^{-1}}$on pos side) 1264 Lya (dv = -238 $\mathrm{km\,s^{-1}}$on pos side) 2020 Lya (dv = 518 $\mathrm{km\,s^{-1}}$on pos side)
HE0429-5343 at 256 kpc, 60deg az:
1167 Lya (dv = -335 $\mathrm{km\,s^{-1}}$on neg side) 1358 Lya (dv = -144 $\mathrm{km\,s^{-1}}$on neg side)
HE0435-5304 at 396 kpc, 62deg az:
1512 Lya (dv = 12 $\mathrm{km\,s^{-1}}$on neg side) 1633 Lya (dv = 131 $\mathrm{km\,s^{-1}}$on neg side) 1690 Lya (dv = 188 $\mathrm{km\,s^{-1}}$on neg side)
RBS567 at 423 kpc, 69deg az:
1664 Lya (dv = 162 $\mathrm{km\,s^{-1}}$on neg side)
HE0439-5254 at 459 kpc, 65deg az:
1148 Lya (dv = -354 $\mathrm{km\,s^{-1}}$on neg side) 1649 Lya (dv = 147 $\mathrm{km\,s^{-1}}$on neg side)

3.0.6. *NGC3513*

Systemic velocity as published: 1194 Velocity as measured: 1203.7 ± 12.0 Rotation velocity (inc corrected) 20 ± 22 $\mathrm{km\,s^{-1}}$Rotation velocity (observed) 11 ± 9 $\mathrm{km\,s^{-1}}$Inclination: 30 Adjusted Inc: 30 Morphology: SB(s)c_HII $L_* = 0.49$

One sightline:
H1101-232 at 60 kpc, 67deg az:
1182 Lya (dv = -22 $\mathrm{km\,s^{-1}}$on pos side)

3.0.7. *NGC3633*

Several locations show two velocities for emission. We have combined these into a single velocity measurement via a weighted average. We measure a redshift for this galaxy of $cz = 2597.6 \pm 2.4$ $\mathrm{km\,s^{-1}}$.

We measure a line-of-sight rotation velocity for NGC3633 of $v_{rot} = 139 \pm 3.3, \ -160 \pm 5.7,$ $\mathrm{km\,s^{-1}}$.

Systemic velocity as published: 2600 Velocity as measured: 2587.2 ± 6.6 Rotation velocity (inc corrected) 157 ± 11 $\mathrm{km\,s^{-1}}$Rotation velocity (observed) 149 ± 6 $\mathrm{km\,s^{-1}}$Inclination: 69 Adjusted Inc: 72 Morphology: SAa $L_* = 0.88$

Three sightlines:
SDSSJ112005.00+041323.0 at 468 kpc, 78deg az:
2285 Lya (dv = -302 $\mathrm{km\,s^{-1}}$on neg side) 2578 Lya (dv = -9 $\mathrm{km\,s^{-1}}$on neg side)
RX_J1121.2+0326 at 184 kpc, 58deg az:
2605 Lya (dv = 18 $\mathrm{km\,s^{-1}}$on neg side)
SDSSJ112224.10+031802.0 at 413 kpc, 50deg az:
Nothing

3.0.8. *NGC4536*

The data on the receding side of NGC4536 is very messy, and may include contamination from background sources.

Systemic velocity as published: 1808 Velocity as measured: 1866.9 ± 32.9 Rotation velocity (inc corrected) 139 ± 37 $\mathrm{km\,s^{-1}}$Rotation velocity (observed) 129 ± 32 $\mathrm{km\,s^{-1}}$Inclination: 59 Adjusted Inc: 61 Morphology: SAB(rs)bc $L_* = 2.0$

Three sightlines:
3C273.0 at 349 kpc, 11deg az:
1580 Lya (dv = -287 $\mathrm{km\,s^{-1}}$on pos side) 2156 Lya (dv = 289 $\mathrm{km\,s^{-1}}$on pos side) 2267 Lya (dv = 400 $\mathrm{km\,s^{-1}}$on pos side)
HE1228+0131 at 338 kpc, 51deg az:
1495 Lya (dv = -372 $\mathrm{km\,s^{-1}}$on pos side) 1571 Lya (dv = -296 $\mathrm{km\,s^{-1}}$on pos side) 1686 Lya (dv = -181 $\mathrm{km\,s^{-1}}$on pos side) 1721 Lya (dv = -146 $\mathrm{km\,s^{-1}}$on pos side) 1854 Lya (dv = -13 $\mathrm{km\,s^{-1}}$on pos side) 2311 Lya (dv = 444 $\mathrm{km\,s^{-1}}$on pos side)
SDSSJ123748.99+012607.0 at 294 kpc, 37deg az:
not finished

3.0.9. *NGC4939*

Systemic velocity as published: 3110 Velocity as measured: 3092.8 ± 33 Rotation velocity (inc corrected) 275 ± 49 $\mathrm{km\,s^{-1}}$Rotation velocity (observed) 204 ± 25 $\mathrm{km\,s^{-1}}$Inclination: 46 Adjusted Inc: 48 Morphology: SA(s)bc $L_* = 5.5$

One sightline:
PG1302-102 at 254 kpc, 61deg az:
3448 Lya (dv = 355 $\mathrm{km\,s^{-1}}$on neg side)

3.0.10. *NGC5364*

Systemic velocity as published: 1241 Velocity as measured: 1238.0 ± 16.9 Rotation velocity (inc corrected) 155 ± 27 $\mathrm{km\,s^{-1}}$Rotation velocity (observed) 130 ± 13 $\mathrm{km\,s^{-1}}$Inclination: 55 Adjusted Inc: 57 Morphology: SA(rs)bc $L_* = 1.9$

Two sightline:
SDSSJ135309.50+033328.0 at 519 kpc, 21deg az:
not finished
SDSSJ135726.27+043541.4 at 165 kpc, 84deg az:
1124 Lya (dv = -114 $\mathrm{km\,s^{-1}}$on pos? side) 1296 Lya (dv = 58 $\mathrm{km\,s^{-1}}$on pos? side)

3.0.11. *NGC5786*

Systemic velocity as published: 2998 Velocity as measured: 2974.6 ± 21.5 Rotation velocity (inc corrected) 172 ± 28 $\mathrm{km\,s^{-1}}$Rotation velocity (observed) 156 ± 19 $\mathrm{km\,s^{-1}}$Inclination: 63 Adjusted Inc: 65 Morphology:

(R'_2)SAB(s)bc $L_* = 25$

One sightline:
QSO1500-4140 at 453 kpc, 1deg az:
3141 Lya (dv = 166 $\mathrm{km\,s^{-1}}$on pos side)

3.0.12. *UGC09760*

Systemic velocity as published: 2023 Velocity as measured: 2093.7 ± 15.5 Rotation velocity (inc corrected) 46 ± 16 $\mathrm{km\,s^{-1}}$Rotation velocity (observed) 46 ± 12 $\mathrm{km\,s^{-1}}$Inclination: 85 Adjusted Inc: 90 Morphology: Sd $L_* = 0.17$

Two sightlines:
SDSSJ151237.15+012846.0 at 123 kpc, 90deg az:
2051 Lya (dv = -43 $\mathrm{km\,s^{-1}}$on minor axis. Looks neg side, but extremely close)

3.1. *Ancillary Data*

4. HALO ROTATION MODEL

In order to better understand how QSO sightlines probe intervening velocity structure we have developed a simple halo gas rotation model. This model is seeded by an observed rotation curve (or whatever rotation curve-esque data suits ones fancy). This input curve is then interpolated and extended out to $2R_{vir}$ based on the average velocity of the outer 1/2 radius. Next, we project this interpolated rotation curve onto a plane oriented to a faux QSO sightline identically to the input galaxy-QSO pair orientation. By stacking multiple rotation-planes in the galaxy z-axis direction, we then create a simple cylindrical rotating halo model. Finally, each rotation-plane in the stack is projected onto the faux sightline. The result is a function representing the rotation velocity encountered by the sightline as a function of velocity (or distance) along it.

For each galaxy-QSO pair we created 3 rotation models: 1) a purely cylindrical halo extending $1R_{vir}$ in height and $2R_{vir}$ in radius, 2) a spherical halo extending $2R_{vir}$ in radius, and 3) a cylindrical model extending $1R_{vir}$ in height and $2R_{vir}$ in radius with rotation velocities which smoothly decline to systemic towards these boundaries.

5. RESULTS

6. SUMMARY

- First result

This research has made use of the NASA/IPAC Extragalactic Database (NED) which is operated by the Jet Propulsion Laboratory, California Institute of Technology, under contract with the National Aeronautics and Space Administration. Based on observations with the NASA/ESA *Hubble Space Telescope*, obtained at the Space Telescope Science Institute (STScI), which is operated by the Association of Universities for Research in Astronomy, Inc., under NASA contract NAS 5-26555. **SALT ACKNOWLEDGEMENT**. Spectra were retrieved from the Barbara A. Mikulski Archive for Space Telescopes (MAST) at STScI. Over the course of this study, D.M.F. and B.P.W. were supported by grant AST-1108913, awarded by the US National Science Foundation, and by NASA grants *HST*-AR-12842.01-A, *HST*-AR-13893.01-A, and *HST*-GO-14240 (STScI).

HST (COS)

$Target$	$Galaxy$	R_{vir} (kpc)	v_{galaxy} (km s^{-1})	$Inc.$ (deg)	$Az.$ [deg]	ρ (kpc)	$v_{Ly\alpha}$ (km s^{-1})	$W_{Ly\alpha}$ (km s^{-1})	Δv (km s^{-1})	$\mathcal{L}$
(1)	(2)	(3)	(4)	(5)	(6)	(7)	(8)	(9)	(10)	(11)
1H0717+714	UGC03804	173	2887	55	7	207	2870	343±6	17	0.24

Table 3
All associated systems. The largest $\mathcal{L}$ value is given, with a (*) indicating that this corresponds to $\mathcal{L}_{d^{1.5}}$, otherwise the quoted $\mathcal{L}$ was computed with R_{vir}.

Statistic	Blueshifted Absorbers	Redshifted Absorbers
Number	22	26
Mean EW [mÅ]	329 ± 52	245 ± 34

Table 4
Average properties of the associated galaxy sample split into red and blue-shifted bins based on Δv.